Journal of Magnetism and Magnetic Materials 427 (2017) 81–84

Contents lists available at ScienceDirect

Journal of Magnetism and Magnetic Materials

journal homepage: www.elsevier.com/locate/jmmm

Biofilm disruption with rotating microrods enhances antimicrobial efficacy

Lamar O. Mair[a,*], Aleksandar Nacev[a], Ryan Hilaman[a], Pavel Y. Stepanov[a], Sagar Chowdhury[a], Sahar Jafari[a], Jeffrey Hausfeld[b], Amy J. Karlsson[c], Mark E. Shirtliff[d], Benjamin Shapiro[e], Irving N. Weinberg[a]

[a] Weinberg Medical Physics, Inc., North Bethesda, MD, USA
[b] School of Medicine and Health Sciences, George Washington University, WA, USA
[c] Department of Chemical and Biomolecular Engineering, University of Maryland, College Park, MD, USA
[d] School of Dentistry, University of Maryland, Baltimore, MD, USA
[e] Fischell Department of Bioengineering, University of Maryland, College Park, MD, USA

ARTICLE INFO

Keywords:
Magnetic microrods
Biofilm
Noncontact manipulation
Infectious disease
Aspergillus

ABSTRACT

Biofilms are a common and persistent cause of numerous illnesses. Compared to planktonic microbes, biofilm residing cells often demonstrate significant resistance to antimicrobial agents. Thus, methods for dislodging cells from the biofilm may increase the antimicrobial susceptibility of such cells, and serve as a mechanical means of increasing antimicrobial efficacy. Using *Aspergillus fumigatus* as a model microbe, we magnetically rotate microrods in and around biofilm. We show that such rods can improve the efficacy of antimicrobial Amphotericin B treatments *in vitro*. This work represents a first step in using kinetic magnetic particle therapy for disrupting fungal biofilms.

1. Introduction

Microbial biofilms are believed to be associated with a broad variety of infectious diseases (e.g., sinusitis, skin ulcers). New methods of preventing and combating these tenacious microbial havens are becoming increasingly important [1]. One characteristic of biofilms that makes them particularly difficult to treat is their increased resistance to antimicrobial therapy [2]. While free-floating microbes may be susceptible to a specific drug or therapy, biofilms of the same microbe often prove drug resistant due to a confluence of factors. The dense meshwork of polysaccharides that mechanically buttresses the biofilm [3] and the evolution of persister cells capable of resisting antimicrobial attack [4] are among the many defenses biofilms may evolve [2]. New approaches, such as dispersal agents and microbial interference, are currently being developed for treating biofilm-associated infections [1, 5, 6].

Aspergillus fumigatus (*A. fumigatus*) is a globally pervasive saprophytic mold that has been implicated in numerous respiratory diseases [7–9]. The spores of *A. fumigatus* are typically spherical in shape, with diameters between 2 μm and 3 μm [10]. *A. fumigatus* has been implicated in numerous respiratory tract diseases, including aspergillosis, invasive pulmonary aspergilloma, immunoglobulin mediated allergic rhinitis, and chronic necrotizing pneumonia [11]. Additionally, *A. fumigatus* produces cytotoxic and immunosuppressive proteins that allow it to live for long periods in the respiratory tract [7]. Proteases produced by *A. fumigatus* have been shown to damage epithelial tissue, and toxins produced by the mold can inhibit ciliary activity, making clearance of the invading microbes difficult [12]. *A. fumigatus* is known to form biofilms [13,14], and these biofilms have demonstrated reduced antifugal drug susceptibility [9].

Using *A. fumigatus* as a model biofilm, we attempted to determine whether biofilms could be disrupted mechanically using rotating magnetic microrods (under control of a magnetic field applied by electromagnet arrays). Previous research has implemented such rod motion for cell alignment [15], cell manipulation [16–18], and high frequency micromotors [19,20].

2. Experimental procedure

2.1. Magnetic microrods

Microrod dimensions were chosen such that the rods were similar in size to the fungal spores. Gold-iron-gold microrods were electroplated into the pores of anodized aluminum oxide membranes (AAO, Whatman Anodisc) with ~250 nm diameter pores. AAO membranes were first sealed on one side by thermal evaporation of a silver working electrode. After sealing one side, a gold layer (~10 nm) was deposited from commercial gold plating solution (Technic Inc.); iron was

* Corresponding author.
E-mail address: Lamar.Mair@gmail.com (L.O. Mair).

http://dx.doi.org/10.1016/j.jmmm.2016.10.100
Received 25 June 2016; Received in revised form 18 October 2016; Accepted 19 October 2016
Available online 21 October 2016
0304-8853/

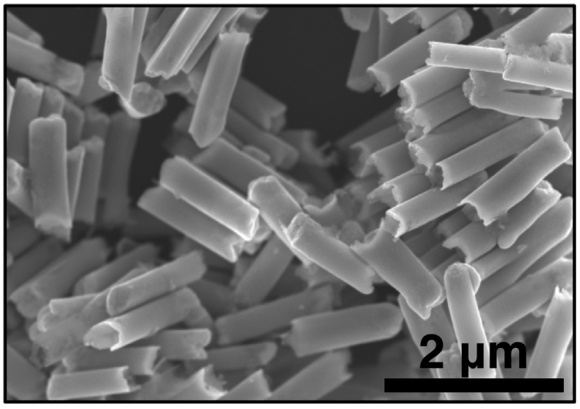

Fig. 1. SEM image of Au-Fe-Au microrods.

electroplated from a solution containing 140 g/l $FeSO_4$-$7H_2O$, 5 g/l $FeCl_3$-$6H_2O$, 45 g/l H_3BO_3, and 2 g/l ascorbic acid, using DC voltage [21]. Our rods were deposited using 1.2 V DC at a current of 0.4 mA. A capping layer of gold (~10 nm) was plated. Rods were approximately 1.2 μm long (Fig. 1). After growth, the silver working electrode was etched in dilute nitric acid and the AAO template was etched in 1 M sodium hydroxide. Detailed synthesis procedures have been well documented in the literature [22–27].

2.2. *Aspergillus fumigatus* culture

Aspergillus fumigatus cells (American Type Cell Culture #10894) were grown on glass cover slips (#1 thickness, 22 mm×22 mm) coated with potato dextrose agar. Cultures were grown for 10 days at 25 °C prior to treatments.

2.3. Treatments

A. fumigatus cultures were divided into four treatment groups (Groups A through D) and each group was challenged with one of four treatment regimens (Fig. 2). Treatments were delivered in 0.1 ml aliquots. All treatments were delivered in phosphate buffered saline (PBS). In Fig. 2, PBS (treatment carrier fluid) is shown in yellow. Group A received phosphate buffered saline only (control). Group B received the antifungal Amphotericin B (AmpB) only. The Amphotericin B dose was 750 ng (in 0.1 ml PBS), less than the intranasal doses given in clinical trials [28]. Group C received ~100,000 rotating microrods. Group D received combined antifungal (750 ng AmpB) and ~100,000 rotating microrods. Rods were rotated using a magnetic field of ~10 mT and a frequency of 10 Hz.

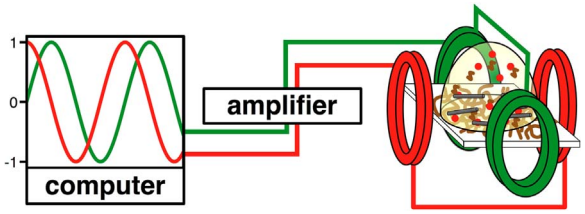

Fig. 3. Apparatus used to manipulate microrods. A computer-generated signal is amplified before reaching two orthogonally arranged Helmholtz coils. Magnetic fields rotate the particles in the plane of the sample.

The magnetic actuation apparatus consisted of two pairs of Helmholtz coils. Signals were generated using Matlab and amplified via audio amplifiers (Fig. 3). The electromagnets generated a rotating magnetic field in the plane of the sample, and microrods rotated in the plane of the fungal cell culture. As they are actuated, microrods interact with *A. fumigatus* cells, underlying potato dextrose agar growth surfaces, and extracellular matrix materials involved in adhering the hyphae of *A. fumigatus* to one another and to surfaces [8].

Following a 20 min treatment period, the supernatant from fluid treatments was extracted. Microrods were magnetically separated from the extracted supernatant fluids. Supernatant fluids were cultured on potato dextrose agar coated petri dishes. The method of counting colony-forming units (CFUs) was used to determine the number of viable cells contained in the supernatant of each treatment group [29].

3. Results

In samples containing microrods, we observed microrod rotation in phase with the applied magnetic field. Microrods formed chains as they rotated, and stirred the fluidic environment. Fig. 4 shows *A. fumigatus* biofilm in the presence of rotating microrods.

Culturing the extracted treatment fluid from Groups A, B, and C resulted in large quantities of viable colony-forming units in these groups ($78.3\times10^6 \pm 32.7\times10^6$, $84\times10^6 \pm 26.6\times10^6$, and $67.7\times10^6 \pm 12\times10^6$ CFU/ml, respectively). Significantly reduced CFUs ($5.33\times10^6 \pm 1.5\times10^6$ CFU/ml) were observed in the group treated with both microrods and antifungal AmpB. CFU results are shown in Fig. 5. Overall, combined microrod disruption and AmpB treatment demonstrated > 90% kill rate, as compared to control, AmpB, or magnetically rotated microrods alone. We observed collisions of the rods with *A. fumigatus* hyphae, leading to disruption of the biofilm integrity.

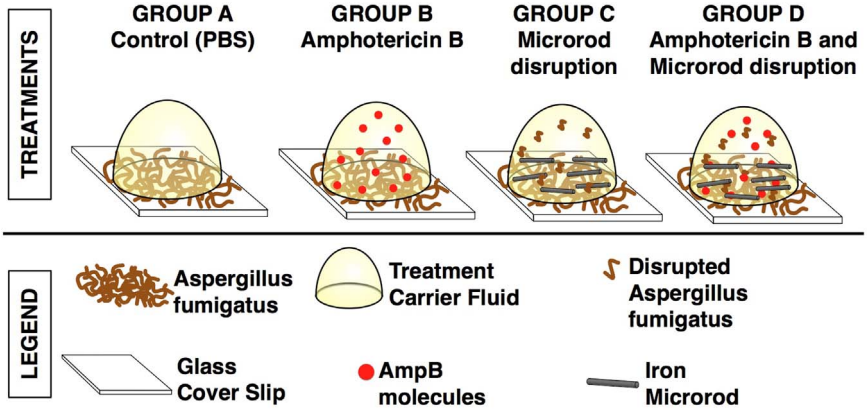

Fig. 2. Four treatments (Groups A through D) were tested on biofilms of *A. fumigatus*. Biofilms were grown on glass cover slips coated with potato dextrose agar. For all experiments, treatment carrier fluid was deposited onto the biofilm and recovered after 20 min of interaction. Cartoon of experiments shows treatment groups. From left to right, treatments group are: PBS only (Group A): Amphotericin B (Group B); microrod disruption (Group C); and combined Amphotericin B and microrod disruption (Group D). (For interpretation of the references to color in this figure, the reader is referred to the web version of this article.)

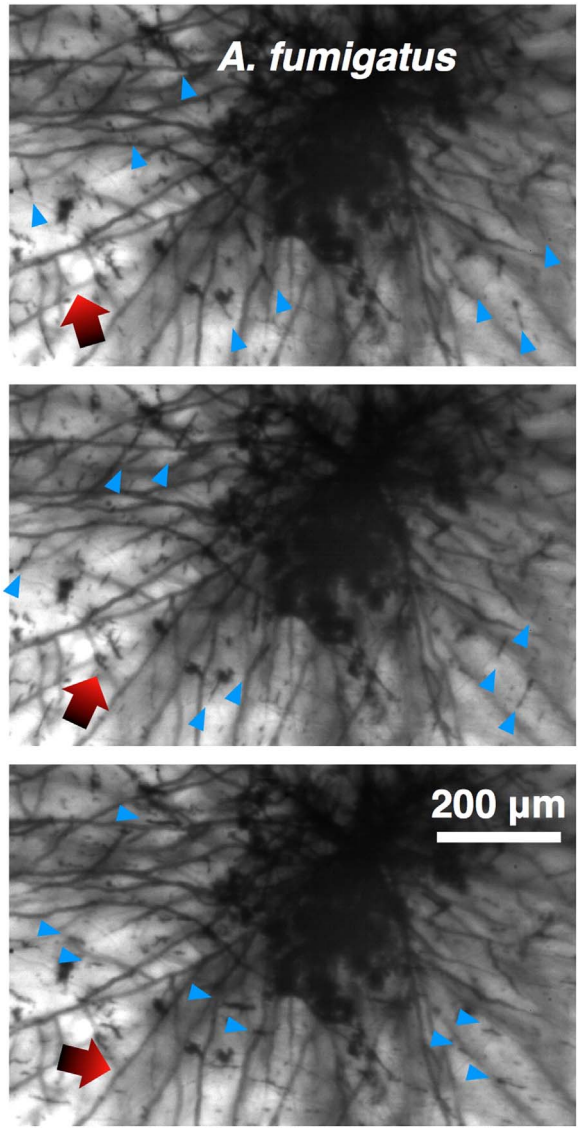

Fig. 4. Microrods rotating in and around *A. fumigatus* hyphae. Red arrows indicate the direction of the applied magnetic field. Blue triangles point to chains of rods aligned with the applied magnetic field. Microrods align, forming chains extending tens to hundreds of micrometers. (For interpretation of the references to color in this figure legend, the reader is referred to the web version of this article.)

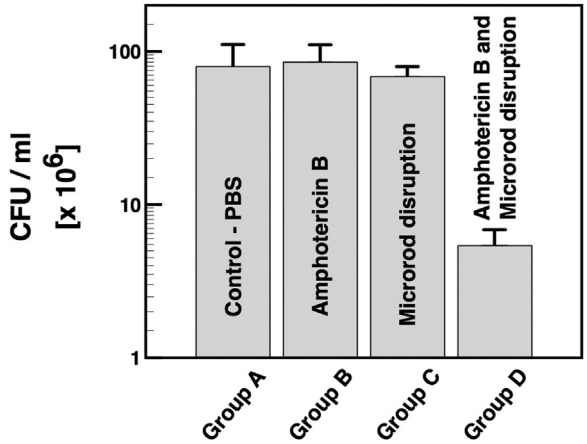

Fig. 5. Using the colony forming unit (CFU) method, we quantified the number of viable colonies contained in the extracted treatment fluids. The CFU data clearly demonstrates the efficacy of combined amphotericin B and microrod disruption treatment.

4. Discussion

These preliminary experiments achieve an order of magnitude reduction in CFUs/ml for magnetically rotated rods potentiating effectiveness of antimicrobial drug. AmpB is not known for being highly efficacious against *Aspergillus* species and in this preliminary study was administered at doses below those administered commonly for therapeutic use [30]. Most antifungal medications have side effects that limit the doses that can be applied clinically (e.g., in patients with renal disease), so it might be useful to have methods of potentiating low-dose administrations [31]. Further work is needed to determine the optimal conditions for synergy between rotating microrods and concomitant medications. Some investigators have found that metallic particles can cause cytotoxic oxidation to human bronchial epithelial cells in the early hours after exposure [32]. Others have used superparamagnetc iron oxide nanoparticles (SPIONs) to suppress biofilm growth, and proposed two potential mechanisms of action [33]. One mechanism relied on SPIONs binding to bacterial cell surfaces, while the other mechanism relied on SPIONs entering bacterial cells. In our experiments, microrods were magnetically separated from the supernatant prior to culturing fungi and performing CFU experiments. In separating fungal cells prior to CFU culture, we anticipate that some fungal cells were also separated from the solution and thus were not included in the solutions used for CFU studies. Thus, we do not anticipate that cell surface binding or cell phagocytosis of particles plays a major role in the CFU data collected. Other reports have shown that using SPIONs for hyperthermic treatments of biofilms result in biofilm dispersal and enhanced antibiotic efficacy [6,34]. The magnetic fields and actuation frequencies used in our study are insufficient to induce hyperthermia. Thus we do not expect that heating played a role in increasing the efficacy of AmpB. Future experiments will probe cytotoxicity in both fungal and mammalian cell lines, and include experiments aimed at optimizing particle size for microbial disruption.

Another possible reason for increased therapeutic efficacy may be better mixing. Rotating magnetic microrods stir the treatment and may increase AmpB efficacy by maximizing the number of disrupted fungal cells exposed to the drug. Previous reports rotated magnetic microrods in the vicinity of blood clots [35]. Adding tissue plasminogen activator, a protein involved in the breakdown of blood clots, to the solution resulted in a two-fold increase in clot thrombolysis [35].

Our group and others have explored image-guided application of magnetic particles to various disease states, including cancer [36]. Gradient coils (operating at much higher field strengths and slew rates than typical MRI systems) can be used to image pathology with high spatial resolution and to direct therapy at these trouble spots (mediated by magnetic particles) [37]. To our knowledge, this is the first application of magnetically rotated microrods for delivering kinetic therapy to challenge fungi implicated in infectious disease. Potential clinical applications include chronic refractory sinusitis, a condition affecting tens of millions worldwide [38]. An even more common condition in which biofilms prevent effective therapy (sometimes leading to amputation) is decubitus or pressure ulcers [39]. Future studies aim to use rotating microrods, positioned and manipulated under image-guidance, to target biofilms *in vivo*. We are currently building a system that can be used to image and manipulate particles [40] for treating sinusitis and other infectious diseases under MRI guidance (Fig. 6). The coils are capable of interleaving magnetic pulses for magnetic resonance imaging, as well as magnetic fields and gradients for manipulating particles.

5. Conclusion

By magnetically rotating microrods in the vicinity of biofilms in a solution containing antimicrobial medication, we demonstrate increased efficacy of Amphotericin B, as compared with treatments of Amphotericin B alone. This work represents a first step in the

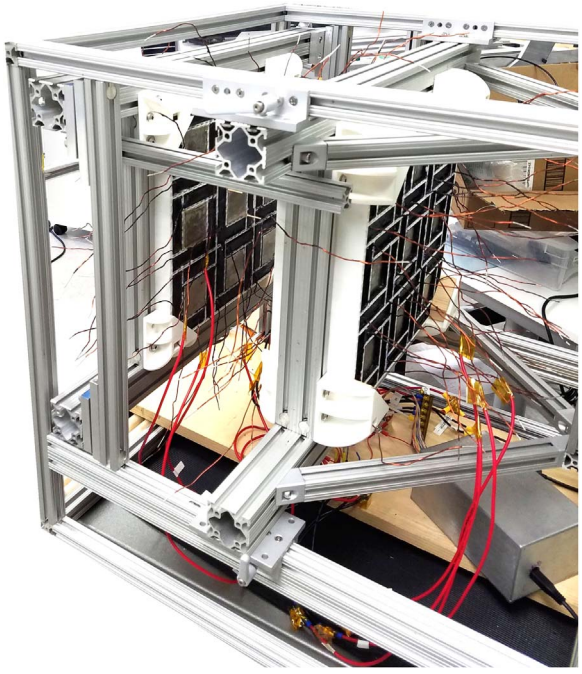

Fig. 6. Arrays of electropermanent magnets have been developed for magnetic resonance imaging and particle manipulation.

validation of image-guided magnetic particle therapy aimed at improving the care of patients with infections.

Acknowledgments

We acknowledge the support of the Maryland NanoCenter, its FabLab, and its AIMLab. We also acknowledge the support of the Georgetown Nanoscience and Microtechnology Lab.

References

[1] S.R. Shah, A.M. Tatara, R.N. D'Souza, A.G. Mikos, F.K. Kasper, Evolving strategies for preventing biofilm on implantable materials, Mater. Today 16 (2013) 177–182.
[2] G. Ramage, R. Rajendran, L. Sherry, C. Williams, Fungal biofilm resistance, Int. J. Microbiol. 2012 (2012).
[3] J.W. Costerton, Z. Lewandowsi, D.E. Caldwell, D.R. Korber, H.M. Lappin-Scott, Microbial biofilms, Annu. Rev. Microbiol. 49 (1995) 711–745.
[4] G. Ramage, E. Mowat, B. Jones, C. Williams, J. Lopez-Ribot, Our current understanding of fungal biofilms, Crit. Rev. Microbiol. 35 (2009) 340–355.
[5] E. Taylor, T.J. Webster, Reducing infections through nanotechnology and nanoparticles, Int. J. Nanomed. 6 (2011) 1463–1473.
[6] T.-K. Nguyen, H.T.T. Duong, R. Selvanayagam, C. Boyer, N. Barraud, Iron oxide nanoparticle-mediated hyperthermia stimulates dispersal in bacterial biofilms and enhances antibiotic efficacy, Sci. Rep. 5 (2015) 18385.
[7] J.P. Latgé, The pathobiology of Aspergillus fumigatus, Trends Microbiol. 9 (2001) 382–389.
[8] A. Beauvais, et al., An extracellular matrix glues together the aerial-grown hyphae of Aspergillus fumigatus, Cell. Microbiol. 9 (2007) 1588–1600.
[9] M.J. Seidler, S. Salvenmoser, F.-M.C. Muller, Aspergillus fumigatus forms biofilms with reduced antifungal drug susceptibility on bronchial pithelial cells, Antimicrob. Agents Chemother. 52 (2008) 4130–4136.
[10] A.Brakhage, B.Jahn, A.Schmidt, Aspergillus fumigatus, Chapter 1: J.B. Georg W., Fresenius and the Description of the Species Aspergillus fumigatus, 1999.
[11] M.J. Seidler, S. Salvenmoser, F.-M.C. Muller, F.-M.C. Müller, Aspergillus fumigatus forms biofilms with reduced antifungal drug susceptibility on bronchial epithelial cells, Antimicrob. Agents Chemother. 52 (2008) 4130–4136.
[12] R. Amitani, et al., Purification and characterization of factors produced by Aspergillus fumigatus which affect human ciliated respiratory epithelium 63 (1995) 3266–3271.
[13] D. Singhal, L. Baker, P.-J. Wormald, L. Tan, Aspergillus fumigatus biofilm on primary human sinonasal epithelial culture, Am. J. Rhinol. Allergy 25 (2011) 219–225.
[14] S. Kaur, S. Singh, Biofilm formation by Aspergillus fumigatus, Med. Mycol. 52 (2014) 2–9.
[15] M. Tanase, et al., Assembly of multicellular constructs and microarrays of cells using magnetic nanowires, Lab Chip 5 (2005) 598–605.
[16] A. Hultgren, M. Tanase, C.S.S. Chen, G.J.J. Meyer, D.H.H. Reich, Cell manipulation using magnetic nanowires, J. Appl. Phys. 93 (2003) 7554–7556.
[17] A. Hultgren, et al., Optimization of yield in magnetic cell separations using nickel nanowires of different lengths, Biotechnol. Prog. 21 (2005) 509–515.
[18] L.O. Mair, et al., Highly controllable near-surface swimming of magnetic Janus nanorods: application to payload capture and manipulation, J. Phys. D: Appl. Phys. 44 (2011) 125001.
[19] D.L. Fan, F.Q. Zhu, R.C. Cammarata, C.L. Chien, Controllable high-speed rotation of nanowires, Phys. Rev. Lett. 247208 (2005).
[20] K. Kim, X. Xu, J. Guo, D.L.L. Fan, Ultrahigh-speed rotating nanoelectromechanical system devices assembled from nanoscale building blocks, Nat. Commun. 5 (2014) 3632.
[21] J. Qin, et al., Differences in the magnetic properties of Co, Fe, and Ni 250-300 nm wide nanowires electrodeposited in amorphous anodized alumina templates, Chem. Mater. 17 (2005) 1829–1834.
[22] R.M. Penner, C.R. Martin, Preparation and electrochemical characterization of ultramicroelectrode ensembles, Anal. Chem. 59 (1987) 2625–2630.
[23] C.R. Martin, Nanomaterials: a membrane-based approach synthetic approach, Science (80-.) 266 (1994) 1961–1966.
[24] A. Fert, L. Piraux, magnetic nanowires, J. Magn. Magn. Mater. 200 (1999) 338–358.
[25] S.J. Hurst, E.K. Payne, L. Qin, C. a. Mirkin, Multisegmented one-dimensional nanorods prepared by hard-template synthetic methods, Angew. Chem. Int. Ed. 45 (2006) 2672–2692.
[26] D. Borissov, S. Isik-uppenkamp, M. Rohwerder, Fabrication of iron nanowire arrays by electrodeposition into porous alumina, J. Phys. Chem. C 113 (2009) 3133–3138.
[27] V. Haehnel, et al., Towards smooth and pure iron nanowires grown by electrodeposition in self-organized alumina membranes, Acta Mater. 58 (2010) 2330–2337.
[28] J.U. Ponikau, D.A. Sherris, A. Weaver, H. Kita, Treatment of chronic rhinosinusitis with intranasal amphotericin B: a randomized, placebo-controlled, double-blind pilot trial, J. Allergy Clin. Immunol. 115 (2005) 125–131.
[29] a.a. Miles, S.S. Misra, J.O. Irwin, The estimation of the bactericidal power of the blood, J. Hyg. 38 (1938) 732–749.
[30] S. Day, et al., Activity of antibiotis against fusarium and aspergillus, Br. J. Opthamol. 93 (2009) 116–119.
[31] S. Bajwa, A. Kulshrestha, Fungal infections in intensive care unit: challenges in diagnosis and management, Ann. Med. Health Sci. Res. 3 (2013) 238–244.
[32] C.R. Keenan, R. Goth-Goldstein, D. Lucas, D.L. Sedlak, Oxidative stress induced by zero-valent iron nanoparticles and Fe(II) in human bronchial epithelial cells, Environ. Sci. Technol. 43 (2009) 4555–4560.
[33] E.N. Taylor, et al., Superparamagnetic iron oxide nanoparticles (SPION) for the treatment of antibiotic-resistant biofilms, Small 8 (2012) 3016–3027.
[34] M.H. Kim, et al., Magnetic nanoparticle targeted hyperthermia of cutaneous staphylococcus aureus infection, Ann. Biomed. Eng. 41 (2012) 598–609.
[35] R. Cheng, et al., Acceleration of Tissue Plasminogen Activator Mediated Thrombolysis by Magnetically Powered Nanomotors, ACS Nano (**8**) (2014) 7746–7754.
[36] J.-B.Mathieu, S.Martel, Magnetic steering of iron oxide microparticles using propulsion gradient coils in MRI, in: Proceedings of the IEEE EMBS Annual International Conference, 2006.
[37] A. Nacev et al., A quiet, fast, high-resolution desktop MRI capable of imaging solids, in: Proceedings of the ISMRM 4833, 2014
[38] D.L. Hamilos, Chronic rhinosinusitis: epidemiology and medical management, J. Allergy Clin. Immunol. 128 (2011) (693–707–709).
[39] D.M. Smith, et al., Evaluation of the bacterial diversity of pressure ulcers using bTEFAP pyrosequencing, BMC Med. Genom. 3 (2010) 41.
[40] A. Nacev, et al., Ultra-Fast MRI for magnetic particle manipulation and imaging, in: Proceedings of the 11th International Conference on the Scientific and Clinical Applications of Magnetic Carriers, Vancouver, Canada, May 31–June 4, 2016.